

## Ordered Mesoporous Copper Oxide with Crystalline Walls\*\*

Xiaoyong Lai, Xiaotian Li,\* Wangchang Geng, Jinchun Tu, Jixue Li, and Shilun Qiu

There is intense interest in the preparation of mesoporous transition-metal oxides possessing a highly ordered pore structure with large specific surface area due to their possible application in areas including catalysis, sorption, chemical and biological separation, photonic and electronic devices, and drug delivery.<sup>[1]</sup> Several mesoporous transition-metal oxides have been prepared, including  $\text{TiO}_2$ ,  $\text{ZrO}_2$ ,  $\text{Nb}_2\text{O}_5$ ,  $\text{WO}_3$ ,  $\text{MnO}_x$ ,  $\text{Ta}_2\text{O}_5$ ,  $\text{V}_2\text{O}_5$ ,  $\text{NiO}$ ,  $\text{CrO}_x$ ,  $\text{Fe}_2\text{O}_3$ , and  $\text{Co}_3\text{O}_4$ ,<sup>[2,3]</sup> although mesoporous copper oxides are of particular interest. Copper oxides are a well known component of catalysts and are widely employed commercially for the direct decomposition of  $\text{N}_2\text{O}$  to  $\text{N}_2$ ,<sup>[4]</sup> CO oxidation,<sup>[5]</sup> and the complete combustion of hydrocarbons.<sup>[6]</sup> Mesoporous copper oxides with an ordered mesoporous structure, large specific surface area, and crystalline walls are expected to provide enhanced catalytic performance in the above-mentioned reactions since they can be regarded as self-supported catalysts with a high activity due to their large specific surface area and a certain degree of size and shape selectivity. In addition, they are also potentially useful as electrode materials in lithium-ion batteries, as their regular porosity would permit intimate flooding of the electrolyte within the particles, and their crystalline walls could be important in promoting lithium intercalation.<sup>[7]</sup> However, to the best of our knowledge no ordered mesoporous copper oxides have been synthesized directly, although it has been possible to prepare unstable lamellar phases of copper oxide.<sup>[8]</sup> Herein, we describe the first synthesis of a mesoporous copper oxide with a periodically ordered uniform pore system, narrow pore-size distribution, and crystalline walls.

The conventional synthesis of ordered mesoporous materials—the utilization of simple and direct sol-gel chemistry—has some difficulties when it comes to transition-metal oxide products. One difficulty is a facile crystallization of most of these oxides, which is accompanied by structural collapse, during mesostructure formation and removal of the organic

templates.<sup>[9]</sup> Moreover, the walls of these mesoporous materials are almost amorphous or semi-crystalline,<sup>[2]</sup> which could limit their wider application in nanotechnology.<sup>[10]</sup> An attractive alternative is the nanocasting method, which has been widely used to synthesize CMK-type carbons.<sup>[11,12]</sup> Such methods employ an ordered mesoporous silica as a rigid template into which a solution-based precursor of the desired phase is introduced. Subsequent heating to form the desired phase and removal of the silica template by leaching with NaOH or HF solution leaves a replica mesoporous structure of the target compound. Several mesoporous transition-metal oxides with crystalline walls have been successfully synthesized by this one-step nanocasting method.<sup>[3]</sup> However, this method also has its limitations, and the leaching of the silica typically affects the material that has been filled into the silica pore system. This problem can be circumvented by not using ordered mesoporous silica as the template but instead to go one step further and use ordered mesoporous carbon formed from the ordered mesoporous silica as template since a carbon template is easily removed by combustion or other methods.<sup>[13,14]</sup> In the present work we utilize a highly ordered mesoporous silica SBA-15 as the template for a highly ordered mesoporous carbon CMK-3 and then obtain ordered mesoporous copper oxide from the CMK-3 by the “one-step-further” nanocasting method.

Figure 1 shows the low-angle powder X-ray diffraction (XRD) patterns of the template SBA-15, CMK-3, and the mesoporous copper oxide. All the XRD patterns have a very sharp diffraction peak and two or more weak peaks, which are characteristic of a 2D hexagonal ( $P6mm$ ) structure.<sup>[15,16]</sup> Although the broadening of the 100 peak in Figure 1c reveals that there is some decrease in structural order during the replication from SBA-15 to the mesoporous copper oxide via CMK-3, three weak but obvious 110, 200, and 210 diffraction peaks indicate a long-range periodic order with hexagonal symmetry in the resultant mesoporous copper oxide material, as confirmed by the transmission electron microscope (TEM) images (see below). It is very interesting that the mesoporous copper oxide obtained from the ordered mesoporous carbon CMK-3 exhibits a highly ordered 2D hexagonal structure, which confirms that a positive replica of SBA-15 has been successfully obtained via two negative replications by the nanocasting method and that the structural order has been maintained.

The wide-angle powder XRD pattern of the mesoporous copper oxide (Figure 2) shows several well-resolved peaks that can be indexed as 110,  $\bar{1}11$ , 111,  $\bar{1}12$ ,  $\bar{2}02$ , 020, 202,  $\bar{1}13$ ,  $\bar{3}11$ , 220, 311, 004, etc., in agreement with the monoclinic phase of CuO (tenorite; powder diffraction file (PDF-2) entry: 48-1548), which indicates that the as-synthesized mesoporous copper oxide has highly crystalline walls.

[\*] X. Lai, Prof. X. Li, W. Geng, J. Tu  
Department of Materials Science  
Jilin University  
Changchun, 130012 (P.R. China)  
Fax: (+86) 431-516-8444  
E-mail: xiaotianli@jlu.edu.cn

Prof. J. Li, Prof. S. Qiu  
State Key Laboratory of Inorganic Synthesis and Preparative Chemistry  
Jilin University  
Changchun, 130012 (P.R. China)

[\*\*] This work was supported by the National Natural Science Foundation of China (grant no. 20151001) and the Natural Science Foundation of Jilin province, China (grant no. 20040505).

Supporting Information for this article is available on the WWW under <http://www.angewandte.org> or from the author.

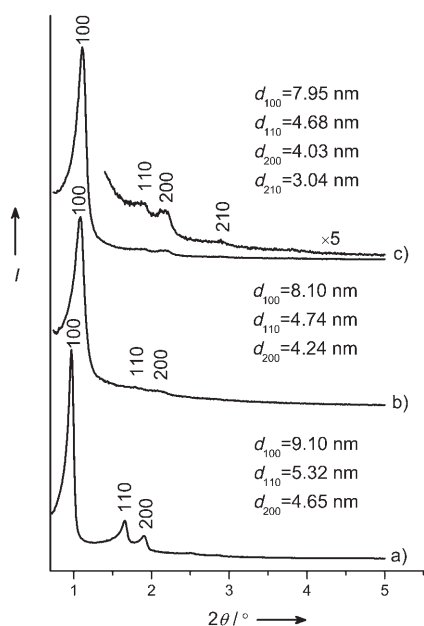


**Figure 1.** Low-angle powder XRD patterns of a) SBA-15, b) CMK-3 synthesized from the SBA-15 in (a), and c) mesoporous copper oxide obtained from the CMK-3 in (b).

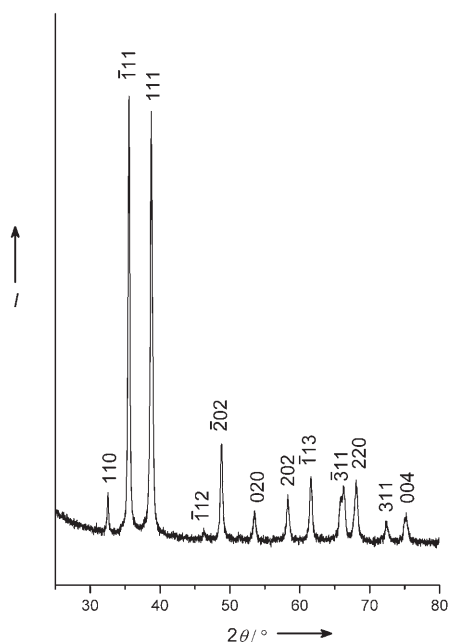


**Figure 2.** Wide-angle powder XRD pattern of the mesoporous copper oxide.

A TEM image of the ordered mesoporous copper oxide was recorded along the  $[001]$  direction (Figure 3a), which confirms a hexagonal structure over a large area. Examination of a wide range of particles demonstrated that they all have similar structures. Combining these results with the TEM image recorded along the  $[110]$  direction (Figure 3b) led to the conclusion that the resultant mesoporous copper

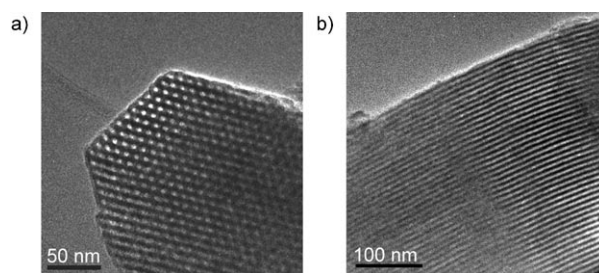


**Figure 3.** TEM image of the mesoporous copper oxide recorded along the a)  $[001]$  and b)  $[110]$  directions.

oxide has a large-scale highly ordered 2D hexagonal array of mesopores, similar to those typically observed in 2D hexagonal mesoporous silica materials such as MCM-41 and SBA-15, in agreement with the XRD data (Figure 1). The TEM image recorded along the  $[110]$  direction also confirmed that the mesoporosity exists throughout the particles, not just near the surface regions. The lattice parameter (9.2–9.4 nm) observed by TEM corresponds well with that calculated from the  $d_{100}$  spacing in the XRD pattern (Table 1).

Figure 4 shows  $N_2$  adsorption–desorption isotherms and the corresponding pore size distribution curve for mesoporous copper oxide. The isotherm has the characteristic type-IV shape and is similar to those of the SBA-15 and CMK-3 template materials (not shown). The mesoporous copper oxide obtained from CMK-3 exhibits a narrow pore-size distribution, and the pore size distribution curve shows a mesopore with a pore size of 5.46 nm at maximum distribu-

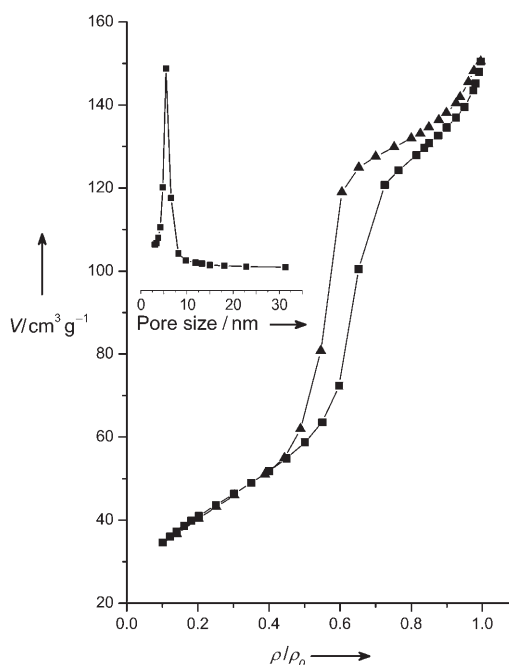


**Figure 4.**  $N_2$  adsorption (■)–desorption (▲) isotherm and corresponding pore size distribution curve (inset) for the mesoporous copper oxide.

**Table 1:** Physical properties of SBA-15, CMK-3, and the mesoporous copper oxide.

Product	Lattice parameter <sup>[a]</sup> [nm]	Surface area <sup>[b]</sup> [m <sup>2</sup> g <sup>-1</sup> ]	Pore volume [cm <sup>3</sup> g <sup>-1</sup> ]	Pore size <sup>[c]</sup> [nm]	Wall thickness <sup>[d]</sup> [nm]
SBA-15	10.51	592	0.89	6.24	4.27
CMK-3	9.35	927	1.40	4.15	–
CuO	9.18	149	0.22	5.46	3.72

[a] Lattice parameter calculated from the  $d_{100}$  spacing in the XRD patterns. [b] Surface area calculated by the BET method. [c] Pore size obtained from the N<sub>2</sub> adsorption isotherms by the BJH method. [d] Wall thickness calculated by subtraction of the pore size from the lattice parameter.

tion. The physical properties of all three products, SBA-15, CMK-3, and mesoporous copper oxide, are shown in Table 1. A decrease in the lattice parameters of these products can be expected due to the thermal treatment at high temperatures.<sup>[14]</sup> The pore size of CMK-3 is very similar to the wall thicknesses of SBA-15 and the mesoporous copper oxide. These results once again indicate the perfect replications from silica to carbon and from carbon to copper oxide. The mesoporous copper oxide has a relatively lower specific surface area and total pore volume than SBA-15, mainly due to the fact that the density of bulk copper oxide is higher than that of bulk silica (6.49 and 2.26 g cm<sup>-3</sup>, respectively). In addition, the above-mentioned partial loss of structural order must also be taken into account.

In conclusion, a novel mesoporous transition-metal oxide with a highly ordered 2D hexagonal structure, in this case mesoporous copper oxide, has been synthesized by using CMK-3 carbon as template. The structure has been confirmed by XRD, TEM, and N<sub>2</sub> adsorption measurements. Such materials have potential applications in catalysis or lithium-ion batteries. Moreover, our study confirms that the “one-step-further” nanocasting method can be extended to ordered mesoporous transition-metal oxide materials. Therefore, it is foreseeable that increasing numbers of mesoporous transition-metal oxide materials with various mesoporous structures will be synthesized by a similar method using mesoporous carbons with different pore connectivities and sizes.

### Experimental Section

Mesoporous silica SBA-15 and mesoporous carbon CMK-3 were obtained following the procedures described elsewhere (see Supporting Information).<sup>[11,15]</sup> In a typical synthesis of mesoporous copper oxide, 2 g of CMK-3 were dispersed in 20 mL of an aqueous solution (0.4 M) of copper nitrate and the mixture heated at 100 °C and stirred for 2 h. The resultant sample was dried under vacuum to give a fine and completely dry powder, then it was slowly heated in a tube furnace under N<sub>2</sub> to 300 °C at a constant rate of 1 °C min<sup>-1</sup> and kept at this temperature for 4 h to convert the copper nitrate within the pores to copper oxide. This procedure was repeated twice. Finally, the sample was calcined in a box furnace at 500 °C for 48 h in air at a heating rate of 1 °C min<sup>-1</sup> to the final temperature to remove the carbon. This treatment gave a black powder in a yield of about 0.8 g of CuO per gram of CMK-3, depending on the pore volume of the CMK-3 template. A lower magnification survey TEM image of the

sample demonstrated that no dense by-product had formed (see Supporting Information).

**Characterization:** Low-angle powder XRD patterns were recorded with a Bruker AXS D8 diffractometer equipped with a Cu<sub>Kα</sub> radiation source (40 kV, 40 mA) with a step width of 0.01° (2θ) and an acquisition time of 4 s per step.

The wide-angle powder XRD pattern was recorded with a Bruker AXS D8 diffractometer equipped with a Cu<sub>Kα</sub> radiation source (40 kV, 40 mA) with a step width of 0.01° (2θ) and an acquisition time of 0.2 s per step.

N<sub>2</sub> adsorption–desorption isotherms were measured with an ASAP 2010 adsorption analyzer (Micromeritics) at –196 °C. Prior to the measurements, all samples were degassed at a temperature of 250 °C for at least 3 h.

TEM images were obtained with a JEOL JEM-3010 microscope operating at 300 kV (coefficient of spherical aberration (C<sub>s</sub>): 0.1 mm; point resolution: 0.14 nm).

Received: August 8, 2006

Published online: December 5, 2006

**Keywords:** copper · materials science · mesoporous materials · oxides · template synthesis

- [1] X. He, D. Antonelli, *Angew. Chem.* **2002**, *114*, 222; *Angew. Chem. Int. Ed.* **2002**, *41*, 214.
- [2] a) P. Yang, D. Zhao, D. I. Margolese, B. F. Chmelka, G. D. Stucky, *Nature* **1998**, *396*, 152; b) Z. Tian, W. Tong, J. Wang, N. Duan, V. V. Krishnan, S. L. Suib, *Science* **1997**, *276*, 926; c) B. Tian, H. Yang, X. Liu, S. Xie, C. Yu, J. Fan, B. Tu, D. Zhao, *Chem. Commun.* **2002**, 1824; d) E. L. Crepaldi, G. J. de A. A. Soler-Illia, D. Grosso, F. Cagnol, F. Ribot, C. Sanchez, *J. Am. Chem. Soc.* **2003**, *125*, 9770; e) N. Ulagappan, C. N. R. Rao, *Chem. Commun.* **1996**, 1685; f) X. Xu, B. Tian, J. Kong, S. Zhang, B. Liu, D. Zhao, *Adv. Mater.* **2003**, *15*, 1932; g) D. M. Antonelli, A. Nakahira, J. Y. Ying, *Inorg. Chem.* **1996**, *35*, 3126; h) D. M. Antonelli, J. Y. Ying, *Chem. Mater.* **1996**, *8*, 874; i) P. Liu, I. L. Moudrakovski, J. Liu, A. Sayari, *Chem. Mater.* **1997**, *9*, 2513; j) S. Banerjee, A. Santhanam, A. Dhathathreyan, P. M. Rao, *Langmuir* **2003**, *19*, 5522; k) A. K. Sinha, K. Suzuki, *Angew. Chem.* **2005**, *117*, 275; *Angew. Chem. Int. Ed.* **2005**, *44*, 271.
- [3] a) F. Jiao, A. Harrison, J. C. Jumas, A. V. Chadwick, W. Kockelmann, P. G. Bruce, *J. Am. Chem. Soc.* **2006**, *128*, 5468; b) B. Z. Tian, X. Y. Liu, L. A. Solovyov, Z. Liu, H. F. Yang, Z. D. Zhang, S. H. Xie, F. Q. Zhang, B. Tu, C. Z. Yu, O. Terasaki, D. Y. Zhao, *J. Am. Chem. Soc.* **2004**, *126*, 865; c) Y. Q. Wang, C. M. Yang, W. Schmidt, B. Spliethoff, E. Bill, F. Schüth, *Adv. Mater.* **2005**, *17*, 53.
- [4] a) G. Centi, S. Perathoner, *Appl. Catal. A* **1995**, *132*, 179; b) A. Dandekar, M. A. Vannice, *Appl. Catal. B* **1999**, *22*, 179; c) M. Matsuoka, W. Ju, K. Takahashi, H. Yamashita, M. Anpo, *J. Phys. Chem. B* **2000**, *104*, 4911.
- [5] A. Martinez-Arias, M. Fernandez-Garcia, O. Galvez, J. M. Coronado, J. A. Anderson, J. C. Conesa, J. Soria, G. Munuera, *J. Catal.* **2000**, *195*, 207.
- [6] J. B. Reitz, E. I. Solomon, *J. Am. Chem. Soc.* **1998**, *120*, 11467.
- [7] a) X. P. Gao, J. L. Bao, G. L. Pan, H. Y. Zhu, P. X. Huang, F. Wu, D. Y. Song, *J. Phys. Chem. B* **2004**, *108*, 5547; b) P. Poizat, S. Laruelle, S. Grugeon, L. Dupon, J. M. Tarascon, *Nature* **2000**, *407*, 496; c) F. Jiao, K. M. Shaju, P. G. Bruce, *Angew. Chem.* **2005**, *117*, 6708; *Angew. Chem. Int. Ed.* **2005**, *44*, 6550.
- [8] P. Yang, D. Zhao, D. I. Margolese, B. F. Chmelka, G. D. Stucky, *Chem. Mater.* **1999**, *11*, 2813.
- [9] F. Schüth, *Chem. Mater.* **2001**, *13*, 3184.
- [10] B. Lee, D. L. Lu, J. N. Kondo, K. Domen, *Chem. Commun.* **2001**, 2118.

- [11] S. Jun, S. H. Joo, R. Ryoo, M. Kruk, M. Jaroniec, Z. Liu, T. Ohsuna, O. Terasaki, *J. Am. Chem. Soc.* **2000**, *122*, 10712.
  - [12] R. Ryoo, S. H. Joo, M. Kruk, M. Jaroniec, *Adv. Mater.* **2001**, *13*, 677.
  - [13] A. H. Lu, W. Schmidt, A. Taguchi, B. Spliethoff, B. Tesche, F. Schüth, *Angew. Chem.* **2002**, *114*, 3639; *Angew. Chem. Int. Ed.* **2002**, *41*, 3489.
  - [14] M. Kang, S. H. Yi, H. I. Lee, J. E. Yie, J. M. Kim, *Chem. Commun.* **2002**, 1944.
  - [15] D. Zhao, J. Feng, Q. Huo, N. Melosh, G. H. Fredrickson, B. F. Chmelka, G. D. Stucky, *Science* **1998**, *279*, 548.
  - [16] C. T. Kresge, M. E. Leonowicz, W. J. Roth, J. C. Vartuli, J. S. Beck, *Nature* **1992**, *359*, 710.
-